

# Pretreatment with Perlecan-Conjugated Laminin-E8 Fragment Enhances Maturation of Grafted Dopaminergic Progenitors in Parkinson's Disease Model

Hiromasa Adachi, Asuka Morizane, Sadaharu Torikoshi, Fabian Raudzus, Yukimasa Taniguchi, Susumu Miyamoto, Kiyotoshi Sekiguchi, Jun Takahashi



The advertisement banner features a dark blue background with a light green horizontal bar at the bottom. On the left, there is a partial view of a white laboratory instrument. The text is centered and reads: "You Don't Need Reproducible Research UNTIL YOU DO." in white, with "UNTIL YOU DO." in a larger font. Below this, the light green bar contains the text "Minimize uncertainty with PHCbi brand products" in white. On the right side of the banner is the PHCbi logo, consisting of the letters "PHCbi" in a bold, blue, sans-serif font, with a small red square above the letter "i".

# Pretreatment with Perlecan-Conjugated Laminin-E8 Fragment Enhances Maturation of Grafted Dopaminergic Progenitors in Parkinson's Disease Model

Hiromasa Adachi<sup>1,2</sup>, Asuka Morizane<sup>1,3,\*</sup>, Sadaharu Torikoshi<sup>1,2</sup>, Fabian Raudzus<sup>1,4,5</sup>, Yukimasa Taniguchi<sup>6</sup>, Susumu Miyamoto<sup>3</sup>, Kiyotoshi Sekiguchi<sup>6,\*</sup>, Jun Takahashi<sup>1,2,\*</sup>

<sup>1</sup>Department of Clinical Application, Center for iPSC Cell Research and Application, Kyoto University, Kyoto, Japan

<sup>2</sup>Department of Neurosurgery, Kyoto University Graduate School of Medicine, Kyoto, Japan

<sup>3</sup>Kobe City Medical Center General Hospital, Center for Clinical Research and Innovation, Hyogo, Japan

<sup>4</sup>Neuronal Signaling and Regeneration Unit, Kyoto University Graduate School of Medicine, Kyoto, Japan

<sup>5</sup>Medical Education Center/International Education Section, Kyoto University Graduate School of Medicine, Kyoto, Japan

<sup>6</sup>Institute for Protein Research, Osaka University, Osaka, Japan

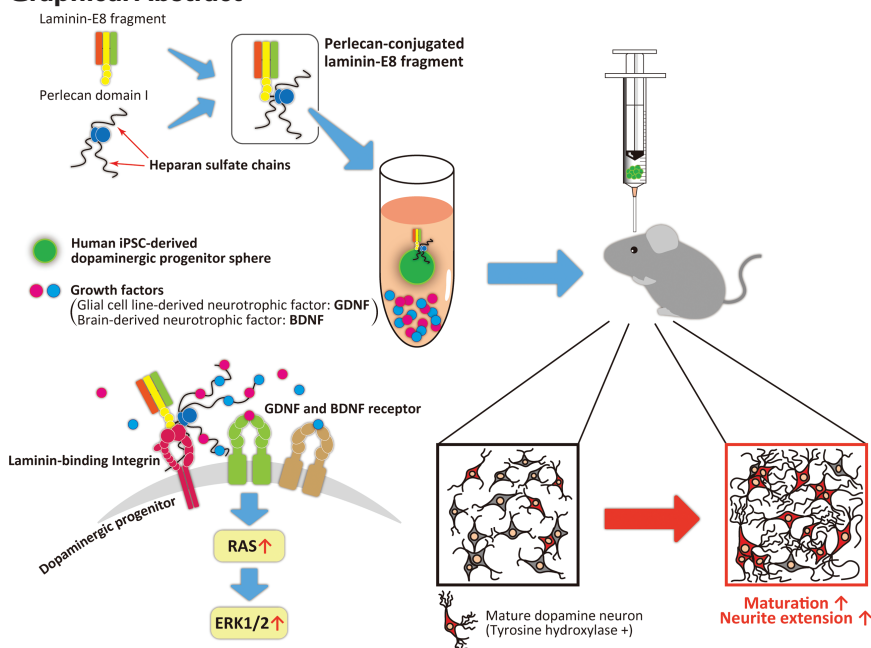
\*Corresponding authors: Asuka Morizane, MD, PhD, Kobe City Medical Center General Hospital, Center for Clinical Research and Innovation, 2-1-1, Minatojima-Minamimachi, Chuo-ku, Kobe, Hyogo 650 0046, Japan. Tel: +81 78 302 4321; Fax: +81 78 302 7537; Email: [morizane@cira.kyoto-u.ac.jp](mailto:morizane@cira.kyoto-u.ac.jp); Jun Takahashi, MD, PhD, Department of Clinical Application, Center for iPSC Cell Research and Application, Kyoto University, 53 Shogoin-Kawahara-cho, Sakyo-ku, Kyoto 606-8507, Japan. Tel: +81 75 366 7052; Fax: +81 75 366 7071; Email: [jbtaka@cira.kyoto-u.ac.jp](mailto:jbtaka@cira.kyoto-u.ac.jp); or, Kiyotoshi Sekiguchi, PhD (for chimeric laminin fragments), Division of Matrixome Research and Application, Institute for Protein Research, Osaka University, 3-2 Yamadaoka, Suita, Osaka 565-0871, Japan. Tel: +81 6 6105 5935; Fax: +81 6 6105 5935; Email: [sekiguch@protein.osaka-u.ac.jp](mailto:sekiguch@protein.osaka-u.ac.jp)

## Abstract

The therapeutic effect of a cell replacement therapy for Parkinson's disease (PD) depends on the proper maturation of grafted dopaminergic (DA) neurons and their functional innervation in the host brain. In the brain, laminin, an extracellular matrix protein, regulates signaling pathways for the survival and development of neurons by interacting with integrins. The heparan sulfate (HS) chain binds mildly to various neurotrophic factors and regulates their intracellular signaling. Perlecan-conjugated laminin 511/521-E8 fragments (p511/p521) were designed to contain an integrin-binding site and HS chains. Here we examined the effect of treating DA progenitors with p511/p521 prior to transplantation in rodent PD models. In vitro and in vivo experiments showed that p511/p521 treatment enhanced the maturation and neurite extension of the grafted DA progenitors by activating RAS-ERK1/2 signaling. This strategy will contribute to an efficient cell replacement therapy for PD in the future.

**Key words:** Parkinson's disease; dopaminergic neurons; cell transplantation; laminin; perlecan.

## Graphical Abstract



Received: 23 December 2021; Accepted: 18 April 2022.

© The Author(s) 2022. Published by Oxford University Press.

This is an Open Access article distributed under the terms of the Creative Commons Attribution-NonCommercial License (<https://creativecommons.org/licenses/by-nc/4.0/>), which permits non-commercial re-use, distribution, and reproduction in any medium, provided the original work is properly cited. For commercial re-use, please contact [journals.permissions@oup.com](mailto:journals.permissions@oup.com).



## Significance Statement

The therapeutic effect of a cell replacement therapy for Parkinson's disease depends on the proper maturation of grafted dopaminergic neurons and their functional innervation in the host brain. This study revealed the potential application of a new generation of laminin, the perlecan-binding laminin-E8 fragment, as an extracellular matrix to promote the maturation and neurite extension of dopaminergic progenitors after transplantation. Furthermore, this effect was mediated by the activation of the RAS-ERK1/2 pathway. This strategy will contribute to an efficient cell replacement therapy for Parkinson's disease in the future.

## Introduction

Parkinson's disease (PD) is a progressive neurodegenerative disorder caused by the loss of dopaminergic (DA) neurons in the midbrain. Pharmacological treatment is standard and effective in the early stages of the disease but becomes less effective as the disease progresses and is associated with severe side effects. As an alternative to this pharmacological treatment is surgical treatments such as deep brain stimulation. However, current pharmacological and surgical therapies are symptomatic. On the other hand, cell replacement therapy is expected to be disease modifying. After many clinical and non-clinical studies on cell therapies using fetal tissues, human pluripotent stem cells, including embryonic stem cells (ESCs) and induced pluripotent stem cells (iPSCs), are being considered as promising sources of donor cells, and several clinical trials are already in progress.

One of the challenges of cell therapies in PD is the survival of functional DA neurons. There are several phases in this therapy to optimize the survival. First, the transplantation procedure causes mechanical stress, hypoxia, hypoglycemia, the production of free radicals, and growth factor deprivation, resulting in apoptosis or anoikis: a type of apoptosis induced by detachment from the extracellular matrix (ECM) or adjacent cells, as occurs in cell dissociation. According to previous reports on fetal tissue transplantation, only 3%-20% of grafted DA neurons survive the procedure.<sup>1</sup> Notably, some reports have shown that donor cells at the progenitor stage survive better than fully mature DA neurons.<sup>2,3</sup> Additionally, treatments with ROCK inhibitor<sup>4</sup> and the antioxidant Lazaroid<sup>5</sup> were reported to inhibit anoikis, improving the survivability of the transplanted cells. Furthermore, the depletion of neurotrophic factors after transplantation leads to apoptotic cell death in the early post-grafting period.<sup>1,6</sup> Especially, brain-derived neurotrophic factor (BDNF)<sup>7,8</sup> and glial cell line-derived neurotrophic factor (GDNF)<sup>9,10</sup> are not only required for the survival of DA neurons but also for their long-term maturation. Secondly, the survived progenitors need to become mature DA neurons in the host brain. Thus, the induction of authentic DA progenitors (DAP) cells from pluripotent stem cells is crucial.<sup>11</sup> Thirdly, these DA neurons should extend neurites and interact appropriately with host neurons through synaptic connections. Escaping from the immunological response is also required. The survival rate of cells that develop into properly matured functional DA neurons in the brain is reported to be approximately 6% for ESC-derived DAPs transplanted into rats<sup>12</sup> and 2.7% for iPSC-derived DAPs transplanted into a primate PD-model.<sup>13</sup>

To improve the outcome of a cell transplantation, we focused on the combination of the ECM of the transplanted cells and growth factors. The ECM not only serves as a scaffold for cell adhesion but also inhibits cell death caused by anoikis and contributes to transmembrane signal transduction from integrin family and cell surface growth factor receptors.<sup>14</sup>

Laminin (LM) and proteoglycan are major components of the ECM. Laminins containing subunit  $\alpha 5$  (LAMA5) support the survival and network formation of neurons.<sup>15</sup> LM511, in particular, has been shown *in vitro* to promote the survival and differentiation of midbrain DA neurons by mediating integrin signaling.<sup>16</sup> In animals, proteoglycans consist of glycosaminoglycan and core proteins. Those that have heparan sulfate (HS) as a glycosaminoglycan are called heparan sulfate proteoglycans (HSPGs).<sup>17</sup> Heparan sulfate proteoglycans control the diffusion of growth factors to establish protein gradients during development. Many reports have focused on HS for its binding ability to basic fibroblast growth factor (FGF), FGF receptor,<sup>18-20</sup> and neurotrophic factors such as BDNF and GDNF.<sup>20-25</sup> Perlecan is a secreted HSPG found in the ECM and binds to many growth factors, including FGFs and VEGFs, which are required during differentiation, tumorigenesis, and angiogenesis.<sup>26,27</sup>

Based on the above, a chimeric protein (perlecan-conjugated LM-E8 fragment) was developed by combining an integrin-binding fragment of LM (LM-E8 fragment) with perlecan domain I (PDI). LM-E8 fragment is a truncated protein consisting of the C-terminal regions of the  $\alpha$ ,  $\beta$ , and  $\gamma$  chains and is a functionally minimal form that fully retains the capability of LM to bind integrins.<sup>28</sup> Notably, LM-E8 fragment has a higher adhesive affinity for human pluripotent stem cells than intact LM and supports vigorous proliferation of the cells.<sup>29</sup> PDI carries several HS chains and an LM-binding site (Fig. 1A). Therefore, perlecan-conjugated LM-E8 fragments are expected to provide a coordinated input of integrin signals through LM and signals from neurotrophic factors that bind to HS. Accordingly, we aimed to increase the efficacy of integrin and neurotrophin signaling pathways involved in neuronal survival and differentiation. Thus, in this study, we examined the effect of perlecan-conjugated LM-E8 fragments in the context of the transplantation of iPSC-derived DAPs.

## Materials and Methods

### Human iPSC Culture

Human iPSCs (1039A1) were maintained on iMatrix-511 (Matrixome)-coated plates in StemFit AK-02N (Ajinomoto).<sup>30</sup> When passaging the cells onto iMatrix-coated plates, the iPSCs were dissociated into single cells with x0.5 TrypLE select (ThermoFisher Scientific) and replated at a density of  $3.0 \times 10^4$  cells per 6-well plate with StemFit medium (Ajinomoto).

### Induction of DAPs from Human iPSCs

Human iPSCs were dissociated into single cells after 10 minutes of incubation with TrypLE select and plated on iMatrix-coated 6-well plates at a density of  $5 \times 10^6$  cells with midbrain floor plate induction medium [GMEM supplemented with 8% KSR, 0.1 mM MEM nonessential

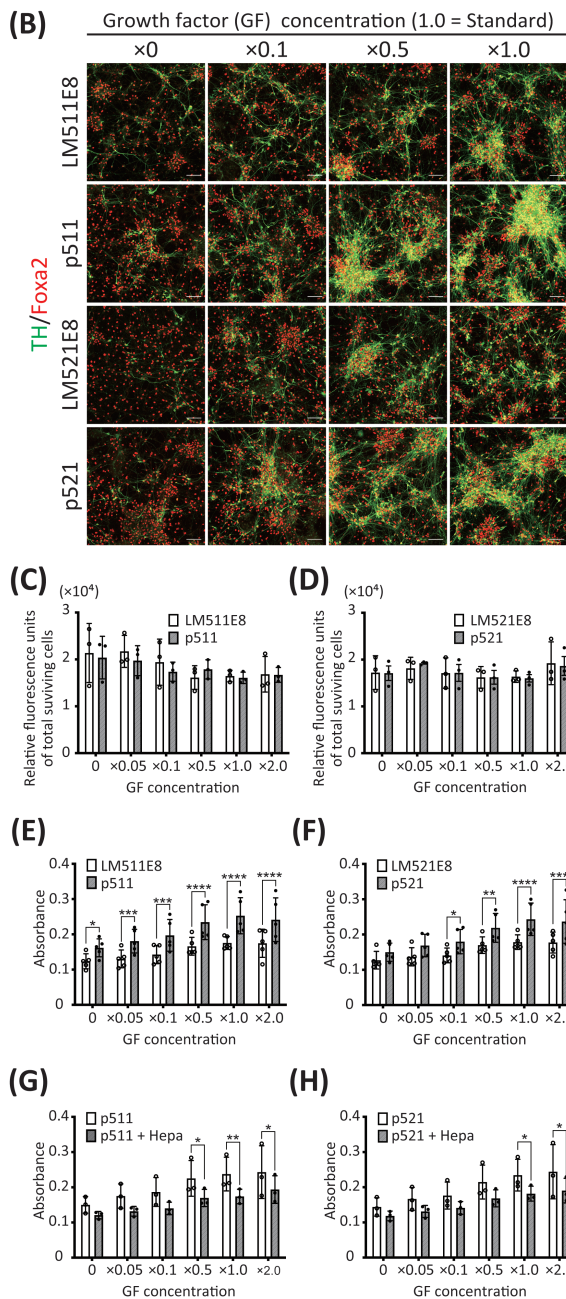
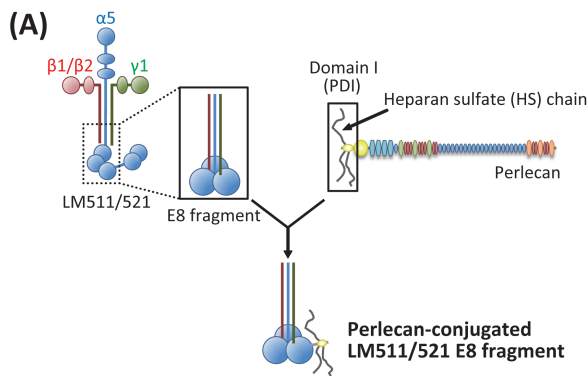


**Figure 1.** Effects of matrix coatings and growth factors in vitro. **(A)** Schematic diagram of LM511/521, E8-fragment, perlecan, and PDI. **(B)** Immunostaining of hiPSC-derived DA neurons (day 42) on different coatings with TH antibody (green) and Foxa2 antibody (red). The growth factor cocktail contains GDNF, BDNF, ascorbic acid, and dibutyryl-cAMP.

amino acids (all ThermoFisher Scientific), sodium pyruvate (Merck), and 0.1 mM mercaptoethanol (Wako)]. We added 100 nM LDN193189 (Stemgent) and 500 nM A83-01 (Wako) to efficiently induce neuronal differentiation.<sup>31</sup> We also added 2  $\mu$ M purmorphamine and 100 ng/mL FGF8 (Wako) from days 1 to 7 and 3  $\mu$ M CHIR99021 (Wako) from days 3 to 12 to induce floor plate cells.<sup>32</sup>

After sorting with anti-Corin antibodies on culture day 12, the sorted cells were replated on low cell adhesion U-bottom 96-well plates (Sumitomo Bakelite) at a density of  $2 \times 10^4$  cells/well for the sphere culture in neural differentiation medium [neurobasal medium supplemented with B27 supplement, 2 mM L-glutamine (all ThermoFisher Scientific), 10 ng/mL GDNF, 20 ng/mL BDNF, 200  $\mu$ M ascorbic acid (all Wako) and 400  $\mu$ M dibutyryl-cAMP (Merck)] as reported previously.<sup>2</sup> To avoid apoptosis at the initial plating, we added 30  $\mu$ M Y-27632 (Wako). For the in vitro experiments,  $5 \times 10^6$  cells/well were replated on 12-well plates without sorting at day 12. After that, we changed the medium every 3 days until the treatment for each experiment on day 28.

### Production of LM-E8 and Perlecan-Conjugated LM-E8 Fragments

Expression vectors for recombinant human LM- $\alpha$ 5E8, LM- $\beta$ 1E8, LM- $\beta$ 2E8, LM- $\gamma$ 1E8, and full-length human perlecan were constructed using a pSecTag2B plasmid as described previously.<sup>33-36</sup> A pcDNA3.4-based expression vector for LM- $\alpha$ 5E8 (pcDNA3.4- $\alpha$ 5E8) was also constructed by inserting the NheI/NotI fragment of pSecTag2B- $\alpha$ 5E8 encoding LM- $\alpha$ 5E8 (Ala2534-Pro3305) into the same restriction sites of pcDNA3.4 (Thermo Fisher Scientific), which had been modified to contain the multicloning site derived from pSecTag2A.<sup>28</sup>

An expression vector for a chimeric protein of LM- $\alpha$ 5E8 (Ala2534-Pro3305) and PDI (Gly25-Pro196), which were connected through a linker segment derived from LM- $\alpha$ 1 (Asp2684-Pro2698), was constructed as follows. cDNA encoding LM- $\alpha$ 5E8 with a C-terminal LM- $\alpha$ 1 linker segment and the cDNA encoding PDI with an N-terminal LM- $\alpha$ 1 linker segment were separately amplified by PCR using expression vectors for LM- $\alpha$ 5E8 and human perlecan as templates and then ligated by extension PCR. The resultant cDNA was cleaved by AscI/NotI and ligated into AscI/NotI-cleaved pcDNA3.4- $\alpha$ 5E8 to generate the expression vector encoding LM- $\alpha$ 5E8-PDI chimeric protein. The DNA sequence was verified using an ABI PRISM 3130xl Genetic Analyzer (Thermo Fisher Scientific).

LM511E8 and LM521E8 were produced using the FreeStyle 293 Expression System (Thermo Fisher Scientific) by transfecting cDNAs encoding LM- $\alpha$ 5E8, LM- $\beta$ 1E8/ $\beta$ 2E8, and LM- $\gamma$ 1E8 into FreeStyle 293-F cells as described

Standard concentration is described as "x1.0" and contains GDNF (10 ng/mL), BDNF (20 ng/mL), ascorbic acid (200  $\mu$ M), and dibutyryl-cAMP (400  $\mu$ M). Scale bars, 100  $\mu$ m. **(C and D)** Number of live cells was measured as fluorescence intensity objectively by the Alamer blue assay. **(E-H)** TH expression level was measured as absorbance objectively by ELISA. **(E and F)** Comparison of LM511E8/LM521E8 and p511/p521. **(G and H)** Heparinase III (Hepa) blocked the effect of the HS chains. Data are represented as the mean  $\pm$  SD,  $n = 5$  (**E and F**) and 3 (**C, D, G and H**) independent experiments. Two-way ANOVA with Bonferroni's multiple comparisons test; \* $P < .05$ , \*\* $P < .01$ , \*\*\* $P < .001$ , \*\*\*\* $P < .0001$ .

previously.<sup>35</sup> Perlecan-conjugated LM511E8 (p511) and LM521E8 (p521) were expressed similarly using the FreeStyle 293 Expression System by transfecting cDNA encoding the LM- $\alpha$ 5E8-PDI chimeric protein instead of LM- $\alpha$ 5E8 cDNA. The recombinant proteins secreted into the culture medium were purified by sequential chromatography on Ni-NTA-agarose (Qiagen) and anti-FLAG M2-agarose (Sigma) columns.<sup>35</sup> The purified proteins were dialyzed against phosphate-buffered saline (pH 7.4), and the protein concentrations were determined using a BCA protein assay kit (Thermo Fisher Scientific) using bovine serum albumin as a standard.

### In Vitro Assay

For in vitro assays, DAPs at day 28 were dissociated, replated at a density  $3.0 \times 10^4$  cells/well on a flat-bottom 96-well plate coated with different matrices (LM511E8, LM521E8, p511, and p521), and cultured in neuronal differentiation media containing GDNF, BDNF, ascorbic acid, and dibutyryl-cAMP until day 42. For HS inhibition experiments, heparinase III (0.5 Sigma unit/mL, Sigma-Aldrich) was added to some wells before seeding the cells and incubating at 37 °C for 2 hours. On day 42, the cells were fixed with 4% paraformaldehyde and stained immunocytochemically with primary antibodies for tyrosine hydroxylase (TH) (Merck) followed by the secondary antibody (donkey anti-rabbit IgG conjugated HRP, Abcam). For high-throughput signal detection, TMB ELISA Substrate Solution and Stop Solution (Abcam) were used. The absorbance was read by an Envision 2104 microplate reader (PerkinElmer) at the 450 nm range and 620 nm as the reference. At the same time, we quantitatively evaluated live cells on day 42 using Alamar blue cell viability reagent (ThermoFisher Scientific). The medium was replaced with medium containing 10% Alamar blue, and the fluorescence intensity (excitation 560 nm, fluorescence 590 nm) was measured after incubating at 37 °C for 3 hours.

### Animal Experiments

All animal procedures described in this study adhered to the guideline for Animal Experiments of Kyoto University and the Guide for the Care and Use of Laboratory Animals of the Institute of Laboratory Animal Resources (ILAR; Washington, DC).

### Pretreatment Before Cell Transplantation

On differentiation day 28, DAP spheres were collected and centrifuged, and the supernatants were removed. The DAP spheres were incubated in neural differentiation medium supplemented with LM511E8/LM521E8 (MW 147 000) or p511/p521 (MW 166 000) after adjusting the molar concentration (LM511E8/LM521E8: 10.0  $\mu$ g/mL, p511/p521: 11.2  $\mu$ g/mL) and with the growth factor cocktail (GDNF, BDNF, ascorbic acid, and dibutyryl-cAMP) for 1 hour at 37 °C just before the transplantation. Also before the transplantation, the samples were centrifuged, and the supernatant was removed. The clumps of spheres were transplanted without dissociation.

### Cell Transplantation into Severe Combined Immunodeficiency Mice

Spheres untreated or treated with LM511E8, LM521E8, p511, or p521 were injected into the striatum of adult severe combined immunodeficiency (SCID) mice (C.B-17/lcrHsd-Prkdcscid,  $n = 8$ ). The cells were injected stereotactically at  $2 \times 10^5$  cells/ $\mu$ L/minute through a 26-G needle. The coordinates were calculated with reference to the Bregma: anterior -0.5 mm, lateral -1.8 mm, ventral -2.5 mm. At 12 weeks after the transplantation, the animals were euthanized with pentobarbital and perfused with 4% paraformaldehyde. The brains were sliced 50- $\mu$ m thick with a cryostat and examined.

### Cell Transplantation into PD Model Rats

Adult athymic nude rats (F344/NJcl-rnu/rnu, CLEA Japan, Inc.) were lesioned in the medial forebrain bundle with 6-hydroxydopamine (6-OHDA) to generate the PD model. The coordinates were calculated with reference to the Bregma: anterior -2.8 mm, lateral -2.0 mm, ventral -7.5 mm. A total of 16  $\mu$ g 6-OHDA per rat in 2.5  $\mu$ L saline with 0.02% ascorbic acid was injected. Five weeks later, all rats were checked for rotational asymmetry by administering methamphetamine (dose of 2.5 mg/kg). Only the rats that showed more than 6 rotations per minute were used as graft recipients, and 20 rats were divided into 3 groups (untreated, p511, and p521) with no rotation bias. Cell transplantation was performed with the stereotactic injection of  $4 \times 10^5$  cells in 2  $\mu$ L (400 000 cells/ $\mu$ L/minute.) through a 22-G needle into the right side of the striatum. The coordinates were calculated with reference to the Bregma: anterior -1 mm, lateral -3 mm, ventral -5 and 4 mm. Twenty weeks after the transplantation, the animals were euthanized with pentobarbital and perfused with 4% paraformaldehyde. The brains were sliced at 50  $\mu$ m thickness with a cryostat and examined.

### Behavioral Analysis

The methamphetamine-induced rotation assay was performed to evaluate behavioral recovery pre-transplantation and every 4 weeks after transplantation using a rotameter apparatus (RotoRat; Med Associates Inc.). A dose of 2.5 mg/kg of methamphetamine (Dainippon Sumitomo Pharma) was injected intraperitoneally, and the rotations were automatically recorded for 90 minutes.

### Active RAS ELISA Assay

DAPs cultured on a LM511E8-coated 12-well plate until day 28 as above were used. On day 28, the DAPs were dissociated and replated at a density of  $1.0 \times 10^6$  cells/well on a 12-well plate coated with different matrices (LM511E8, LM521E8, p511, and p521) and cultured in neuronal differentiation media containing GDNF, BDNF, ascorbic acid, and dibutyryl-cAMP until day 42. The cells were harvested in lysis buffer containing a protease inhibitor and incubated at 4 °C for 15 minutes to detect RAS-ERK1/2 pathway activity downstream of GDNF and BDNF. After centrifugation, the supernatant was collected. Prior to the ELISA, the protein concentration of each sample was adjusted to 50  $\mu$ g/100  $\mu$ L using the Bradford assay (Bio-Rad). We used the RAS GTPase ELISA kit (Abcam) for this analysis. First, we coated a plate with the Glutathione S-Transferase (GST)-fused RAS-binding domain



(RBD) of Raf. EGF-treated HeLa whole-cell extract was used as a positive control. The samples, positive control, and blank were assayed with duplicates. After one hour at room temperature, the wells were washed 3 times, and the primary antibody (rat anti-H-RAS antibody, 1:500) was added to the wells. After another hour at room temperature, the secondary antibody (anti-rat IgG HRP-conjugated, 1:5000) was added after washing 3 times. Finally, after 1 hour at room temperature, the wells were washed 4 times, and chemiluminescent working solution was added. Then, the luminescence intensity was measured using an EnVision2104 microplate reader (PerkinElmer) within 15 minutes. Data were standardized by the value of the positive control.

### Quantitative RT-PCR

Total RNA was isolated using an NucleoSpin RNA XS (Macherey-Nagel), and cDNA was synthesized from 0.4 µg of RNA using PrimeScript RT reagent Kit with gDNA EraserIII (TaKaRa). Quantitative PCR was carried out with Power SYBR Green PCR Master Mix (Thermo Fisher Scientific) and QuantStudio 3 (Thermo Fisher Scientific). The data were assessed using a delta-Ct method and normalized by the glyceraldehyde-3-phosphate dehydrogenase (GAPDH) expression. The primer sequences used are as follows: nuclear receptor subfamily 4 group A member 2 (NR4A2), CGAAACCGAAGAGCCCACAGGA (forward) and GGTCATAGCCGGGTTGGAGTCCG (reverse); and GAPDH, GGTCCGAGTCAACGGATTTG (forward) and TCAGCCTTGACGGTGCCATG (reverse).

### Immunofluorescence Studies

Immunohistochemical analysis of the cryosections was carried out after permeabilization with 0.3% Triton X-200 and 5% normal donkey serum. Immunoreactive cells were observed using a fluorescence microscope (BZ-9000; Keyence) and a confocal laser microscope (LSM 800; Zeiss). The primary antibodies used were as follows: goat anti-Foxa2 (1:500, Santa Cruz Biotechnology), rabbit anti-TH (1:400, Merck), mouse anti-human nuclei (hNuclei, 1:200, Merck), mouse anti-human neural cell adhesion molecule (hNCAM, 1:400, Santa Cruz Biotechnology), mouse anti-LAMA5 (1:200, Abcam), mouse anti-FLAG M2 (1:1000, Merck), rabbit anti-phosphorylated ERK1/2 (pERK, 1:400, Cell Signaling), and rat anti-NR4A2 (1:1000, donated by the KAN laboratory).

### Quantification

Brain slices 50-µm thick were prepared, and every sixth slice was analyzed. In the case of the spheres, samples were thinly sliced at 20 µm and examined. Immunofluorescence images were captured on the LSM 800. The number of TH+, Foxa2+, hNuclei+, and pERK+ cells in the graft were counted manually through all graft images. The graft volume (mm<sup>3</sup>) was quantified by measuring the entire hNuclei+ area in the graft. The innervation of DA neurons originating from the donor cells was quantified by calculating the co-stained area of TH+ and hNCAM+ cells in the striatum. The percentage of innervation was automatically calculated as the ratio of that area to the whole striatum, excluding the graft itself, using the ZEN system (Zeiss). In addition, the value corrected by the number of TH+ cells in the graft was calculated.

### Statistical Analysis

Statistical analysis was performed using a commercially available software package (GraphPad Prism 9; GraphPad Software). Data from the in vitro and in vivo experiments were analyzed by a paired or unpaired *t* test, a one-way ANOVA with Bonferroni's or Dunnett's multiple comparisons analysis, and a 2-way ANOVA with Bonferroni's or Dunnett's multiple comparisons test. Differences with *P* < .05 were considered statistically significant. Data are presented as the mean ± SD or mean ± SEM.

## Results

### Perlecan-Conjugated LM-E8 Fragments (p511/p521) Enhance the Maturation of DAPs in the Presence of Growth Factors

Perlecan-conjugated LM-E8 fragments include the integrin-binding site of LM and HS chains of PDI (Fig. 1A). To investigate the effect of the HS chains on the adhesion culture of DAPs induced from human iPSCs, we analyzed the expression levels of TH and Foxa2, a marker of mesencephalic mature DA neurons, at differentiation day 42.

We examined 2 isoforms of LM, LM511E8 (laminin511-E8 fragment) and LM521E8 (laminin521-E8 fragment), which are well established for the differentiation of DA neurons.<sup>2,37,38</sup> Both isoforms have LAMA5, which has been reported to support the survival and network formation of neurons. Two perlecan-conjugated LM-E8 fragments were prepared using LM511 and LM521: p511 (perlecan-conjugated laminin511-E8 fragment) and p521 (perlecan-conjugated laminin521-E8 fragment). We compared differences among the 4 coating matrices (LM511E8, LM521E8, p511, and p521) from day 28. A cocktail of growth factors with GDNF, BDNF, ascorbic acid, and dibutyl-*c*-AMP was added in graded dilutions to the wells coated with each matrix. The standard concentration of the cocktail used for our DAP differentiation protocol is described as "×1.0": GDNF (10 ng/mL), BDNF (20 ng/mL), ascorbic acid (200 µM), and dibutyl-*c*-AMP (400 µM).

Immunostaining at day 42 showed that TH+Foxa2+ cells were more abundant in p511/p521 than in LM511E8/LM521E8 over different cocktail concentrations (Fig. 1B). Perlecan-conjugation did not increase the number of live cells for LM511E8 or LM521E8 according to an Alamar blue assay for cell quantification (Fig. 1C and 1D). On the other hand, both p511/p521 increased TH expression compared to LM511E8/LM521E8 according to immunocytochemistry and ELISA results (Fig. 1B, 1E, and 1F). To inhibit the effect of the HS chain on perlecan, we additionally treated each matrix with heparinase III, which reduced the TH expression level in the p511/p521 groups to that of the LM511E8/LM521E8 groups (Fig. 1G and 1H).

### Perlecan-Conjugated LM-E8 Fragments (p511/p521) Enhance the Maturation of Transplanted DAPs

To examine the possible application of p511/p521 to cell therapies for PD, DAP donors were pretreated with LM511E8/LM521E8 or p511/p521 and transplanted into SCID mice. As reported previously, we sorted DAPs with anti-Corin antibodies on day 12, continued the culture as floating spheres, and transplanted the cells into SCID mice on day 28 [2]. The

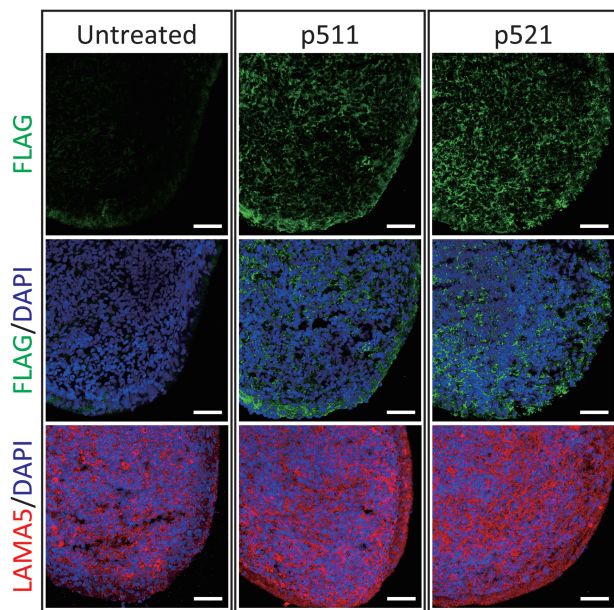


**Figure 2.** Perlecan-conjugated LM E8-fragments (p511/p521) were expressed on the surface and inside of the sphere after pretreatment. Immunostaining images for FLAG tag (attached to the LM subunit  $\gamma$  of p511/p521, green), LAMA5 (red) and DAPI (blue) in spheres on day 28 pretreated with p511/p521 for 1 h, 37 °C. Scale bars, 50  $\mu$ m.

spheres were incubated with LM511E8/LM521E8 or p511/p521 with the standard concentration ( $\times 1.0$ ) of growth factor cocktail for more than 1 hour at 37 °C just before the transplantation. To investigate the distribution and penetration of the matrix by pretreatment of the spheres, we took advantage of the FLAG tag attached to the LM subunit  $\gamma$  of p511/p521. Immunostaining images of the sphere showed FLAG tag was present not only on the surface but also inside the sphere. On the other hand, LAMA5 was diffusely expressed inside all spheres, including untreated spheres (Fig. 2), suggesting that endogenous LM containing LAMA5 was expressed within the neurospheres despite the addition of exogenous LM.

Three months after the transplantation, immunohistochemical analysis was performed (Fig. 3A). The number of survived donor cells positive for the human-specific marker hNuclei and the number of mature DA neurons positive for TH were similar across groups (Fig. 3B and 3C). However, the percentage of mature DA neurons (TH+) among survived cells (hNuclei+) was significantly higher in the p511 group than in the LM511E8 group or untreated group ( $8.9 \pm 0.5\%$ ,  $5.6 \pm 0.4\%$ , and  $6.2 \pm 1.1\%$ , respectively, mean  $\pm$  SD, Fig. 3D). Similarly, in the p521 group, the percentage of TH+ neurons was significantly higher than in the LM521E8 group or untreated group ( $10.3 \pm 1.4\%$ ,  $4.7 \pm 1.3\%$ , and  $6.2 \pm 1.1\%$ , respectively, mean  $\pm$  SD, Fig. 3D).

Next, to evaluate the behavioral recovery and innervation of DA neuron fibers within the striatum, we examined the effect of pretreatment with p511/p521 on 6-OHDA lesioned PD model rats. Five months after the transplantation, immunohistology was performed (Fig. 4A). Resembling the results in mice, the number of hNuclei+ cells and TH+ cells in the grafts were similar across groups (Fig. 4B and 4C), but the percentages of TH+/hNuclei+ (Fig. 4D) and TH+/Foxa2+ (Fig. 4E) cells were significantly higher in the p511/p521 group than in the untreated ones. To estimate neuronal fiber

extensions from the graft, fibers double positive for hNCAM and TH in the striatum, which confirmed these fibers as graft-origin DA neurons, were automatically detected by software (ZEN 2, blue edition, Zeiss). The detected values were greater in the p511/p521 groups than in the untreated group and especially significant in the p521 group (Fig. 4F and 4G). The same results were obtained after correcting for the number of TH+ cells in each group, suggesting that individual DA neurons were fully matured (Fig. 4H). A behavioral assessment after the transplantation using the methamphetamine-induced rotation test showed improvement in all groups at 20 weeks (Fig. 4I).

### Perlecan-Conjugated LM-E8 Fragments (p511/p521) Activate Signaling in the RAS-ERK1/2 Pathway Downstream of GDNF and BDNF

To investigate the downstream signaling changes of GDNF and BDNF by p511/p521, we analyzed the RAS pathway, which plays a crucial role in increasing the TH activity, plasticity, and specificity of DA neurons.<sup>39,40</sup> We quantitatively evaluated activated RAS in DA neurons in vitro on day 42 under p511/p521 coating by ELISA. Interestingly, the levels of RAS activity were significantly increased in the culture under p511/p521-coating compared with LM511E8/LM521E8 coating, respectively (Fig. 5A and 5B). Next, to confirm the activity of the RAS-ERK1/2 pathway in vivo, we analyzed the phosphorylation level of ERK1/2 in the grafts of the SCID mice. pERK is active and transduces signaling to the nucleus. Most TH+ cells were positive for pERK, and the percentage of pERK/hNuclei positive cells was significantly higher in the p511/p521 groups compared with groups that received unconjugated LM or untreated grafts (Fig. 5C and 5D). Since the activated RAS-ERK1/2 pathway is known to promote the expression of NR4A2 [also known as nuclear receptor related 1 protein (NURR1)], which directly activates TH expression in DA neurons, we assessed NR4A2 expression on day 42 under p511/p521 coating. Immunocytochemical analysis showed that p511/p521-coating increased the percentage of NR4A2+ cells among Foxa2+ cells compared with LM511/LM521 coating (Fig. 5E-5G), although no significant difference was shown by RT-qPCR (Fig. 5H and 5I).

## Discussion

This study showed that p511/p521 promotes the maturation but not survival or proliferation of DAPs. In vitro experiments showed that coating with perlecan-conjugated LM increased the number of TH+ cells compared with only LM coating. Titration assays for neurotrophic factors, including GDNF and BDNF, showed the effects of p511/p521 appeared with a higher dose of neurotrophic factors but was inhibited by heparinase III treatment, which specifically cleaves the 1-4 linkage of N-sulfated/N-acetylglucosamine and glucuronic acid to degrade the HS chain into oligosaccharides. Together, these results indicate that the HS chains of p511/p521 enhance the maturation effect of neurotrophic factors on DAPs.

In the transplantation experiments, neither pretreatment with LM511E8/LM521E8 nor p511/p521 changed the total number of surviving transplanted cells (hNuclei+). On the other hand, pretreatment with p511/p521 significantly increased the percentage of TH+/hNuclei+ cells in SCID mice and PD model rats. Furthermore, in PD model rats, neurite



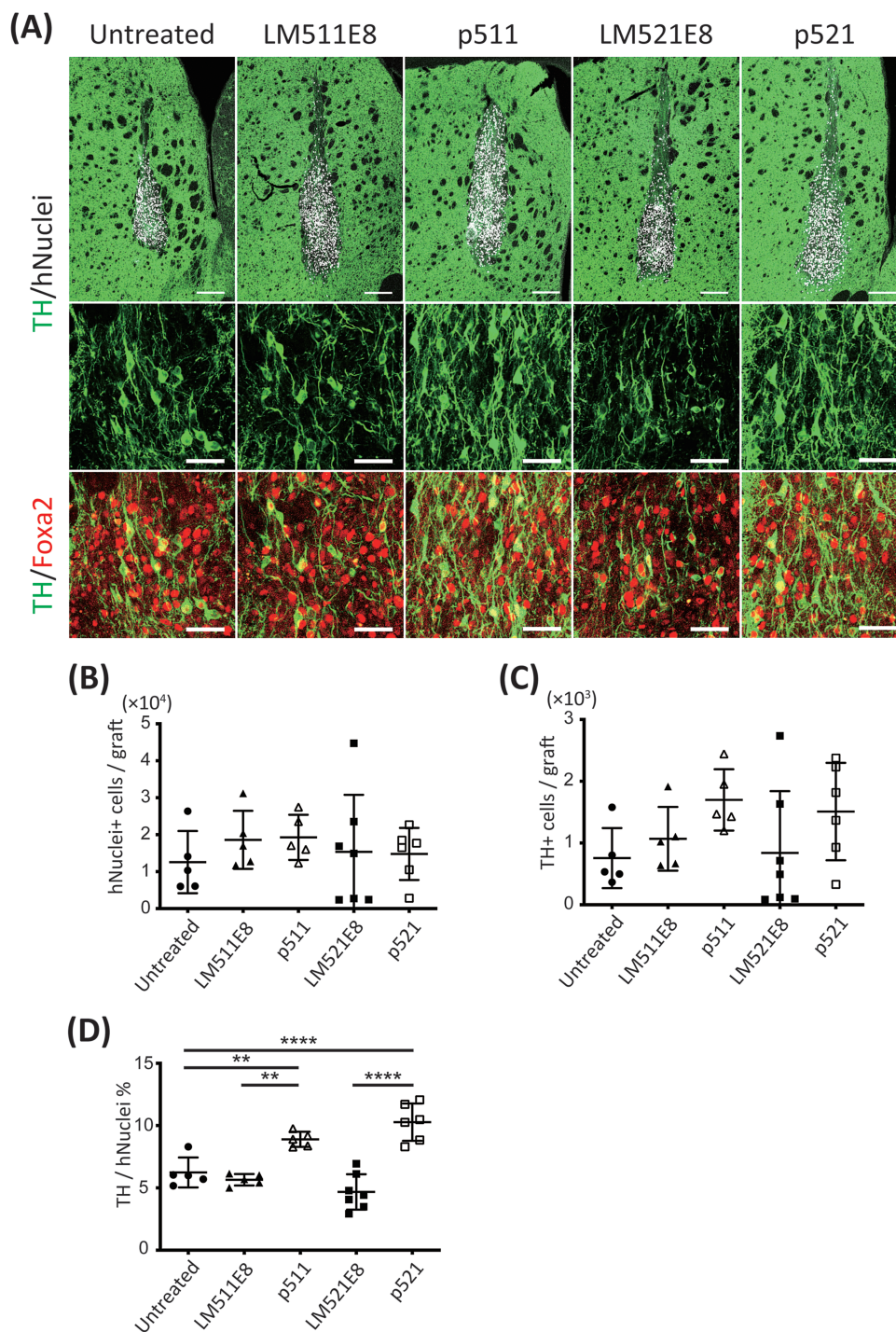


**Figure 3.** Perlecan-conjugated LM E8-fragments (p511/p521) increased the proportion of mature DA neurons within the grafts in SCID mice. **(A)** Immunohistochemistry of the grafts. Scale bars, 200  $\mu\text{m}$  (upper images) and 50  $\mu\text{m}$  (middle and lower images). Number of surviving hNuclei+ donor cells **(B)**, TH+ DA neurons **(C)**, and the percentage of TH+ cells per hNuclei+ cells **(D)**. Data are represented as the mean  $\pm$  SD,  $n = 5-7$ , one-way ANOVA with Bonferroni's multiple comparisons test; \*\* $P < .01$ , \*\*\*\* $P < .0001$ .

outgrowth was enhanced. These results show that the conjugation of HS chains to LM promotes the maturation of DAPs after transplantation.

The immunostaining of spheres pretreated with p511/p521 indicated that the transplanted DAPs were surrounded by the LM fragment, to which HS chains were bound. It was reported that a similar pretreatment procedure had positive effects on muscle cell transplantation using LM-E8 fragment

( $\alpha 3/4/5$ ).<sup>41</sup> Therefore, we hypothesized that intracellular signals from the receptors of neurotrophic factors and integrin can be inputted side-by-side.

We also demonstrated that the maturation-promoting effects by p511/p521 were mediated through RAS-ERK1/2 signaling downstream of GDNF- and BDNF-receptor activation. Within DA neurons, BDNF and GDNF trigger signals through autophosphorylation of the receptor tyrosine

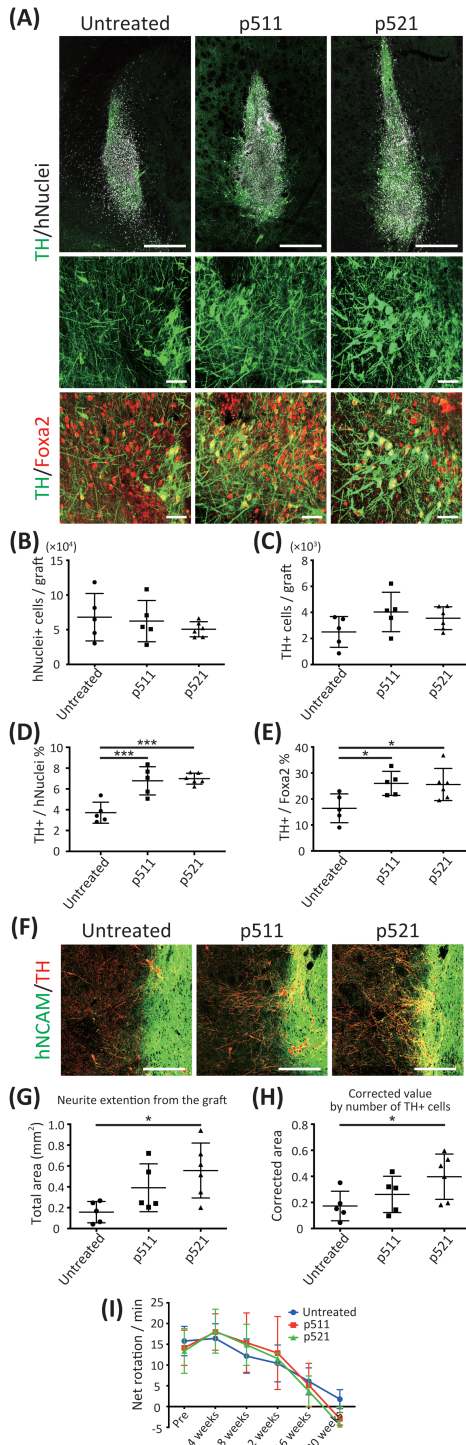


**Figure 4.** Perlecan-conjugated LM E8-fragments (p511/p521) increased the proportion of mature DA neurons within grafts and their neurite outgrowth in PD model rats. **(A)** Immunohistochemistry of the grafts. Scale bars, 500  $\mu$ m (upper images) and 50  $\mu$ m (middle and lower images). Number of surviving hNuclei+ donor cells **(B)**, TH+ DA neurons **(C)**, and the percentage of TH+ cells per hNuclei+ cells **(D)** and per Foxa2+ cells **(E)**. Data are represented as the mean  $\pm$  SD,  $n = 5$  or 6, one-way ANOVA with Dunnett’s multiple comparisons test;  $*P < .05$ ,  $***P < .001$ . **(F)** Immunohistochemistry of the neurite outgrowth from the grafts. Scale bars, 100  $\mu$ m. **(G)** Quantification of neurite extensions from the graft and into the striatum. Neurites positive for both hNCAM and TH were measured as the area (mm<sup>2</sup>). **(H)** Corrected values by the number of TH+ cells. One-way ANOVA, Dunnett’s multiple comparisons test;  $*P < .05$ . **(I)** Evaluation of behavioral recovery using the methamphetamine-induced rotation test every 4 weeks after transplantation. Two-way ANOVA with Dunnett’s multiple comparisons test.

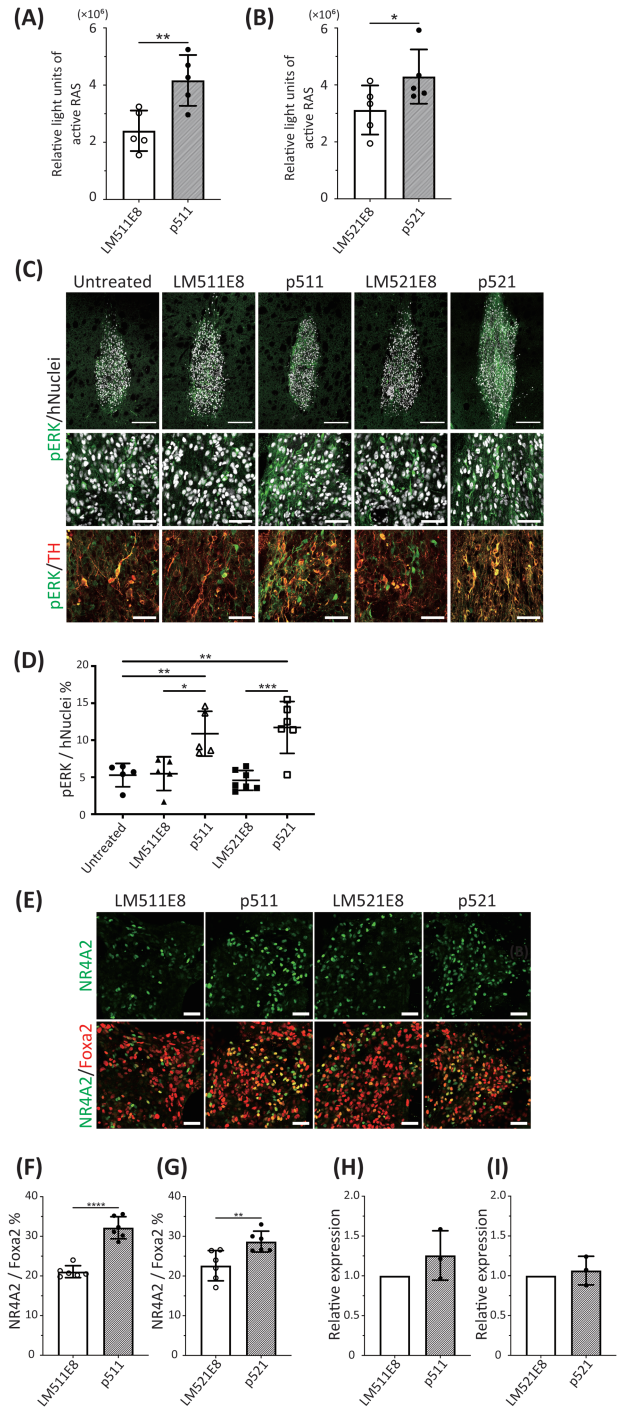


**Figure 5.** Perlecan-conjugated LM E8-fragments (p511/p521) mediated activation of the RAS-ERK1/2 pathway. **(A, B)** Relative level of activated RAS evaluated by ELISA coated with LM511E8/LM521E8 or p511/p521. Data are represented as the mean  $\pm$  SD,  $n = 5$ , independent experiments. Paired  $t$ -test;  $*P < .05$ ,  $**P < .01$ . **(C)** Immunohistochemistry of the grafts transplanted into SCID mice. Scale bars, 200  $\mu$ m (upper images) and 50  $\mu$ m (middle and lower images). **(D)** The percentage of ERK phosphorylated cells to transplanted cells (hNuclei+ cells). Data are represented as the mean  $\pm$  SD,  $n = 5-7$ , one-way ANOVA with Bonferroni’s multiple comparisons test;  $*P < .05$ ,  $**P < .01$ ,  $***P < .001$ . **(E)** Immunostaining images of hiPSC-derived DA neurons (day 42) on 4 different coatings with NR4A2 (NURR1) antibody (green) and Foxa2 antibody (red). **(F, G)** The percentage of NR4A2+ cells per Foxa2+ cells. Data are represented as the mean  $\pm$  SD,  $n = 6$  totally; 3 samples in each of 2 independent experiments. Unpaired  $t$  test;  $**P < .01$ ,  $****P < .0001$ . **(H, I)** NR4A2 expression analysis by quantitative RT-qPCR. The expression level of the cells with LM511E8/LM521E8 was set to 1.0. Data are represented as the mean  $\pm$  SD,  $n = 3$  independent experiments. Unpaired  $t$  test.



kinases TrkB and Ret, respectively. These signals mainly modulate the downstream AKT-PI3K and RAS-MAPK (ERK1/2) pathways.<sup>42,43</sup> Both pathways play an important role in neuronal survival, proliferation, neuronal differentiation, neurite growth, and neuronal regeneration.<sup>44</sup>

We found that activated RAS was elevated in DAPs cultured with p511/p521 and that the phosphorylation of ERK1/2, an indicator of upstream activation of the RAS pathway, was enhanced in the grafts 3 months after transplantation into SCID mice. Enhanced RAS expression leads to an increased number and functional protection of DA neurons.<sup>39,40</sup> The major downstream signaling pathways triggered by RAS activation are the PI3K-AKT-mTOR and RAF-MEK-ERK1/2 cascades.<sup>45</sup> PI3K-AKT signaling plays a major role in cell proliferation and survival by protecting neurons from diverse stress factors.<sup>46,47</sup> The RAF-MEK-ERK1/2 pathway triggers a wide range of cellular responses, including neurite growth, differentiation, inflammation, and apoptosis.<sup>48</sup> However, the mechanisms associated with the cell survival and cytoprotective effects through the RAS-ERK1/2 pathway are poorly understood. Debate remains on whether ERK1/2 interacts directly with the apoptosis machinery, as in the PI3K-AKT pathway, or indirectly through impaired axon outgrowth and reduced access to trophic factors, which may further vary by the type of neuron.<sup>45</sup> It has been reported that activation of the RAS-ERK1/2 pathway, but not the PI3K-AKT pathway, increases the plasticity, specificity, and maturity of DA neurons in the graft.<sup>49</sup> It was also reported that activation of the RAS-ERK1/2 pathway increases the expression of NURR1, which regulates the transcription of TH.<sup>50</sup> That finding is in agreement with our observation that enhancing the RAS-ERK1/2 pathway did not increase the number of surviving cells (hNuclei+ cells) but did increase the percentage of TH+ mature DA neurons.

In order to understand the mechanism of the effect of p511/p521, LM-integrin interactions should be considered. LM-E8 fragment is composed of the C-terminal region of the subunits  $\alpha$ ,  $\beta$ , and  $\gamma$  and contains the active integrin-binding site.<sup>29</sup> Signals from LM conveyed via integrin could affect cell adhesion, differentiation, phenotypic stability, and resistance to anoikis.<sup>15,29,51</sup> Among the LM-binding integrins,  $\alpha 6\beta 1$  and  $\alpha 3\beta 1$  integrins are the major receptors for LM511 and LM521, 2 LM isoforms containing LAMA5.<sup>52,53</sup>  $\alpha 6\beta 1$  integrin induces Fyn-RhoA-ROCK signaling by binding LM and suppressing the ROCK pathway, and  $\alpha 3\beta 1$  integrin selectively activates the PI3K-AKT pathway rather than the RAS-ERK1/2 pathway to strongly enhance cell survival.<sup>53,54</sup> Integrins  $\alpha 3$ ,  $\alpha 6$ , and  $\beta 1$  have been shown to be abundantly expressed in the developing ventral midbrain, where DA neurons are localized.<sup>16</sup> The PI3K-AKT and RAS-ERK1/2 pathways do not work independently but cooperatively with growth factor receptors and integrin signals. Although enhanced RAS signaling may support the survival of the grafted DA neurons, coordinated LM-integrin signaling has a strong suppressive effect on apoptosis via the Fyn-RhoA-ROCK and PI3K-AKT pathways. These effects are equally exerted by perlecan conjugated LM (p511/p521) and unconjugated LM (LM511E8/LM521E8). Hence, there was no difference in the final cell survival after transplantation between the different treatments.

Contrary to our expectations, the effect of pretreatment with unconjugated LM (LM511E8/LM521E8) was not apparent. This result might be due to the form of our donor

cells as neurospheres, which were generated under 3-dimensional culture. Sphere transplantation causes less damage to the cells compared with single-cell transplantation, in which the cells need to be detached from the culture dish enzymatically followed by dissociation and centrifugation before transplantation. Anoikis, which is caused by the preparation and transplant procedure, is a major cause of transplant cell death and occurs within a few days after the transplantation.<sup>1,6</sup> In the case of single-cell transplantations, several methods to encapsulate the DA neurons in a hydrogel made by artificially mimicking ECM (LM, type 1 collagen, hyaluronic acid, etc.) have been reported as effective.<sup>55-58</sup> In addition, it is known that endogenous ECM, including LM, is expressed inside the neurospheres during the culture.<sup>59</sup> We also found a diffuse expression of LAMA5 within the spheres of all groups used for our transplantation, including those that were not pretreated. Therefore, we concluded that endogenous LM in the neurospheres served as a scaffold for cell adhesion and inhibited apoptosis through integrin signaling.

In the present study, we examined 2 LM isoforms, LM511 and LM521. Both isoforms have LAMA5 and have been reported to bind several types of integrins ( $\alpha 6\beta 1$ ,  $\alpha 3\beta 1$ , and  $\alpha 6\beta 4$ ) to support neuronal survival and network formation.<sup>15</sup> They are structurally very similar and have been used to differentiate DA neurons with good results. However, the  $\beta 2$  and  $\beta 1$  subunits differ in their binding affinity for integrins. LM521 binds to  $\alpha 3\beta 1$  integrin with 4 times higher affinity than LM511.<sup>35</sup> Because the neurite extensions originating from the graft in PD model rats were significantly enhanced with LM521 treatment, we suspect the high affinity for  $\alpha 3\beta 1$  integrin is a factor.

Finally, behavioral assessments did not find a significant improvement in the p511/p521 groups, probably because even the untreated groups showed enough surviving DA neurons to improve the motor symptoms.

In conclusion, pretreating iPSC-derived DAPs with p511/p521 activated the RAS-ERK1/2 pathway and promoted their maturation after transplantation in the brain. Further studies are needed to optimize the time and dose for the pretreatment with p511/p521 and to clarify their safety for human use. However, it should be noted that our results are not directly applicable to the transplantation of dissociated cells, because we transplanted the cells as neurospheres. Current clinical trials expect the survival of a minimum of 100 000 mature grafted DA neurons per side, which is about half the normal number of physiological nigrostriatal DA neurons that project to the striatum in humans.<sup>60,61</sup> A recent study in rhesus macaques found that 40 000 to 70 000 mature DA neurons are required in the putamen to recover up to 50% of motor scores; this range is estimated to be approximately 160 000 to 300 000 DA neurons for humans.<sup>62</sup> Thus, pretreatment with p511/p521 may support the efficient maturation of DAPs after transplantation and early recovery of symptoms.

## Acknowledgment

We are indebted to Dr. Peter Karagiannis for editing a draft of this article. We are also grateful to all members of the Takahashi lab for their technical advice and insightful discussions. This study was supported by a grant from the Network Program for Realization of Regenerative Medicine from the Japan

Agency for Medical Research and Development (AMED) and the Takeda Science Foundation.

## Conflict of Interest

Y.T. declared patent holder as one of the inventors of perlecan-conjugated laminin E8 fragments. K.S. declared leadership position with of Matrixome, Inc., one of the inventors of perlecan-conjugated laminin E8 fragments, research funding from Nippi, Inc., and cofounder and a shareholder of Matrixome, Inc. J.T. declares research funding from Sumitomo Dainippon Pharma.

## Author Contributions

H.A.: conception and design, correction and assembly of data, data analysis and interpretation, manuscript writing. A.M.: conception and design, administrative support, final approval of manuscript. S.T.: conception and design, correction and assembly of data, data analysis and interpretation. F.R.: manuscript writing, data analysis and interpretation. Y.T., K.S.: provision of study material, manuscript writing. S.M.: final approval of manuscript. J.T.: conception and design, administrative support, and final approval of manuscript.

## Data Availability

The data that support the findings of this study are available from the corresponding author upon reasonable request.

## References

- Brundin P, Karlsson J, Emgård M, et al. Improving the survival of grafted dopaminergic neurons: a review over current approaches. *Cell Transplant*. 2000;9:179-195. <https://doi.org/10.1177/09636897000900205>.
- Doi D, Samata B, Katsukawa M, et al. Isolation of human induced pluripotent stem cell-derived dopaminergic progenitors by cell sorting for successful transplantation. *Stem Cell Rep*. 2014;2:337-350. <https://doi.org/10.1016/j.stemcr.2014.01.013>.
- Ganat YM, Calder EL, Kriks S, et al. Identification of embryonic stem cell-derived midbrain dopaminergic neurons for engraftment. *J Clin Invest*. 2012;122:2928-2939. <https://doi.org/10.1172/JCI58767>.
- Koyanagi M, Takahashi J, Arakawa Y, et al. Inhibition of the Rho/ROCK pathway reduces apoptosis during transplantation of embryonic stem cell-derived neural precursors. *J Neurosci Res*. 2008;86:270-280. <https://doi.org/10.1002/jnr.21502>.
- Nakao N, Frodl EM, Duan WM, et al. Lazaroids improve the survival of grafted rat embryonic dopamine neurons. *Proc Natl Acad Sci USA*. 1994;91:12408-12412.
- Sortwell CE, Parkinson S. Strategies for the augmentation of grafted dopamine neuron survival Caryl E. Sortwell. *Front Biosci*. 2003;8:522-532.
- Yurek DM, Lu W, Hipkens S, et al. BDNF enhances the functional reinnervation of the striatum by grafted fetal dopamine neurons. *Exp Neurol*. 1996;137:105-118. <https://doi.org/10.1006/exnr.1996.0011>.
- Baquet ZC, Bickford PC, Jones KR. Brain-derived neurotrophic factor is required for the establishment of the proper number of dopaminergic neurons in the substantia nigra pars compacta. *J Neurosci*. 2005;25:6251-6259.
- Redmond DE, McEntire CRS, Kingsbery JP, et al. Comparison of fetal mesencephalic grafts, AAV-delivered GDNF, and both combined in an MPTP-induced nonhuman primate Parkinson's model. *Mol Ther*. 2013;21:2160-2168. <https://doi.org/10.1038/mt.2013.180>.
- Deng X, Liang Y, Lu H, et al. Co-transplantation of GDNF-overexpressing neural stem cells and fetal dopaminergic neurons mitigates motor symptoms in a rat model of Parkinson's disease. *PLoS One*. 2013;8:e808801-e808809. <https://doi.org/10.1371/journal.pone.0080880>.
- Tabar V, Studer L. Pluripotent stem cells in regenerative medicine: challenges and recent progress. *Nat Rev Genet*. 2014;15:82-92. <https://doi.org/10.1038/nrg3563>.
- Kriks S, Shim J-W, Piao J, et al. Floor plate-derived dopamine neurons from hESCs efficiently engraft in animal models of PD. *Nature* 2012;480:547-551.
- Kikuchi T, Morizane A, Doi D, et al. Human iPS cell-derived dopaminergic neurons function in a primate Parkinson's disease model. *Nature* 2017;548:592-596. <https://doi.org/10.1038/nature23664>.
- Kim SH, Turnbull J, Guimond S. Extracellular matrix and cell signalling: The dynamic cooperation of integrin, proteoglycan and growth factor receptor. *J Endocrinol*. 2011;209:139-151. <https://doi.org/10.1530/JOE-10-0377>.
- Hyysalo A, Ristola M, Mäkinen MEL, et al. Laminin  $\alpha 5$  substrates promote survival, network formation and functional development of human pluripotent stem cell-derived neurons in vitro. *Stem Cell Res*. 2017;24:118-127. <https://doi.org/10.1016/j.scr.2017.09.002>.
- Zhang D, Yang S, Toledo EM, et al. Niche-derived laminin-511 promotes midbrain dopaminergic neuron survival and differentiation through YAP. *Sci Signal* 2017;10.
- Sarrazin S, Lamanna WC, Esko JD. Heparan sulfate proteoglycans. *Cold Spring Harb Perspect Biol* 2011;3:1-33.
- Shimokawa K, Kimura-Yoshida C, Nagai N, et al. Cell surface heparan sulfate chains regulate local reception of FGF signaling in the mouse embryo. *Dev Cell*. 2011;21:257-272. <https://doi.org/10.1016/j.devcel.2011.06.027>.
- Bishop JR, Schuksz M, Esko JD. Heparan sulphate proteoglycans fine-tune mammalian physiology. *Nature* 2007;446:1030-1037. <https://doi.org/10.1038/nature05817>.
- Häcker U, Nybakken K, Perrimon N. Heparan sulphate proteoglycans: the sweet side of development. *Nat Rev Mol Cell Biol*. 2005;6:530-541. <https://doi.org/10.1038/nrm1681>.
- Davies JA, Yates EA, Turnbull JE. Structural determinants of heparan sulphate modulation of GDNF signalling. *Growth Factors* 2003;21:109-119. <https://doi.org/10.1080/08977190310001621005>.
- Kanato Y, Ono S, Kitajima K, et al. Complex formation of a brain-derived neurotrophic factor and glycosaminoglycans. *Biosci Biotechnol Biochem*. 2009;73:2735-2741. <https://doi.org/10.1271/bbb.90637>.
- Barnett MW, Fisher CE, Perona-Wright G, et al. Signalling by glial cell line-derived neurotrophic factor (GDNF) requires heparan sulphate glycosaminoglycan. *J Cell Sci*. 2002;115:4495-4503. <https://doi.org/10.1242/jcs.00114>.
- Bespalov MM, Sidorova YA, Tumova S, et al. Heparan sulfate proteoglycan syndecan-3 is a novel receptor for GDNF, neurturin, and artemin. *J Cell Biol*. 2011;192:153-169. <https://doi.org/10.1083/jcb.201009136>.
- Rickard SM, Mummery RS, Mulloy B, et al. The binding of human glial cell line-derived neurotrophic factor to heparin and heparan sulfate: Importance of 2-O-sulfate groups and effect on its interaction with its receptor, GFR $\alpha 1$ . *Glycobiology* 2003;13:419-426. <https://doi.org/10.1093/glycob/cwg046>.
- Gubbiotti MA, Neill T, Iozzo RV. A current view of perlecan in physiology and pathology: a mosaic of functions. *Matrix Biol*. 2017;57:285-298.
- Whitelock JM, Melrose J, Iozzo RV. Diverse cell signaling events modulated by Perlecan. *Biochemistry* 2008;47:11174-11183.
- Takizawa M, Arimori T, Taniguchi Y, et al. Mechanistic basis for the recognition of laminin-511 by  $\alpha 6 \beta 1$  integrin. *Sci Adv*. 2017;3:1-8.
- Miyazaki T, Futaki S, Suemori H, et al. Laminin E8 fragments support efficient adhesion and expansion of dissociated human pluripotent stem cells. *Nat Commun*. 2012;3:1210-1236.

30. Samata B, Doi D, Nishimura K, et al. Purification of functional human ES and iPSC-derived midbrain dopaminergic progenitors using LRTM1. *Nat Commun.* 2016;7:1-11.
31. Morizane A, Doi D, Kikuchi T, et al. Small-molecule inhibitors of bone morphogenic protein and activin/nodal signals promote highly efficient neural induction from human pluripotent stem cells. *J Neurosci Res.* 2011;89:117-126. <https://doi.org/10.1002/jnr.22547>.
32. Kriks S, Shim JW, Piao J, et al. Dopamine neurons derived from human ES cells efficiently engraft in animal models of Parkinson's disease. *Nature* 2011;480:547-551. <https://doi.org/10.1038/nature10648>.
33. Ido H, Nakamura A, Kobayashi R, et al. The requirement of the glutamic acid residue at the third position from the carboxyl termini of the laminin  $\gamma$  chains in integrin binding by laminins. *J Biol Chem.* 2007;282:11144-11154. <https://doi.org/10.1074/jbc.M609402200>.
34. Ido H, Harada K, Yagi Y, et al. Probing the integrin-binding site within the globular domain of laminin-511 with the function-blocking monoclonal antibody 4C7. *Matrix Biol.* 2006;25:112-117. <https://doi.org/10.1016/j.matbio.2005.10.003>.
35. Taniguchi Y, Ido H, Sanzen N, et al. The C-terminal region of laminin  $\beta$  chains modulates the integrin binding affinities of laminins. *J Biol Chem.* 2009;284:7820-7831.
36. Li S, Shimono C, Norioka N, et al. Activin A binds to perlecan through its pro-region that has heparin/heparan sulfate binding activity. *J Biol Chem.* 2010;285:36645-36655.
37. Niclis JC, Gantner CW, Alsanje WF, et al. Efficiently specified ventral midbrain dopamine neurons from human pluripotent stem cells under xeno-free conditions restore motor deficits in Parkinsonian rodents. *Stem Cells Transl Med* 2017;6:937-948.
38. Lu HF, Chai C, Lim TC, et al. A defined xeno-free and feeder-free culture system for the derivation, expansion and direct differentiation of transgene-free patient-specific induced pluripotent stem cells. *Biomaterials* 2014;35:2816-2826.
39. Heumann R, Goemans C, Bartsch D, et al. Transgenic activation of Ras in neurons promotes hypertrophy and protects from lesion-induced degeneration. *J Cell Biol.* 2000;151:1537-1548.
40. Chakrabarty K, Serchov T, Mann SA, et al. Enhancement of dopaminergic properties and protection mediated by neuronal activation of Ras in mouse ventral mesencephalic neurones. *Eur J Neurosci.* 2007;25:1971-1981.
41. Ishii K, Sakurai H, Suzuki N, et al. Recapitulation of extracellular LAMININ environment maintains stemness of satellite cells in vitro. *Stem Cell Rep.* 2018;10:568-582.
42. Palasz E, Wysocka A, Gasiorowska A, et al. BDNF as a promising therapeutic agent in Parkinson's disease. *Int J Mol Sci.* 2020;21.
43. Kramer ER, Liss B. GDNF-Ret signaling in midbrain dopaminergic neurons and its implication for Parkinson disease. *FEBS Lett.* 2015;589:3760-3772.
44. Schöneborn H, Raudzus F, Coppey M, et al. Perspectives of RAS and RHEB GTPase signaling pathways in regenerating brain neurons. *Int J Mol Sci.* 2018;19:1-37.
45. Zhong J. RAS and downstream RAF-MEK and PI3K-AKT signaling in neuronal development, function and dysfunction. *Biol Chem.* 2016;397:215-222.
46. Castellano E, Downward J. Role of RAS in the regulation of PI 3-kinase. In: Rommel C, Vanhaesebroeck B, Vogt PK, eds. *Phosphoinositide 3-kinase Heal. Dis.* Vol. 1, Berlin, Heidelberg: Springer Berlin Heidelberg, 2011:143-169.
47. Nair VD, Olanow CW. Differential modulation of akt/glycogen synthase kinase-3 $\beta$  pathway regulates apoptotic and cytoprotective signaling responses. *J Biol Chem.* 2008;283:15469-15478.
48. Roux PP, Blenis J. ERK and p38 MAPK-activated protein kinases: a family of protein kinases with diverse biological functions. *Microbiol Mol Biol Rev.* 2004;68:320-344.
49. Gantner CW, de Luzy IR, Kauhausen JA, et al. Viral delivery of GDNF promotes functional integration of human stem cell grafts in Parkinson's disease. *Cell Stem Cell* 2020;26:511-526.e5.
50. Kim KS, Kim CH, Hwang DY, et al. Orphan nuclear receptor Nurrl directly transactivates the promoter activity of the tyrosine hydroxylase gene in a cell-specific manner. *J Neurochem.* 2003;85:622-634.
51. Domogatskaya A, Rodin S, Tryggvason K. Functional diversity of laminins. *Annu Rev Cell Dev Biol.* 2012;28:523-553.
52. Nishiuchi R, Takagi J, Hayashi M, et al. Ligand-binding specificities of laminin-binding integrins: a comprehensive survey of laminin-integrin interactions using recombinant  $\alpha 3\beta 1$ ,  $\alpha 6\beta 1$ ,  $\alpha 7\beta 1$  and  $\alpha 6\beta 4$  integrins. *Matrix Biol.* 2006;25:189-197.
53. Nakashima Y, Omasa T. What kind of signaling maintains pluripotency and viability in human-induced pluripotent stem cells cultured on laminin-511 with serum-free medium?. *Biores Open Access.* 2016;5:84-93.
54. Gu J, Fujibayashi A, Yamada KM, et al. Laminin-10/11 and fibronectin differentially prevent apoptosis induced by serum removal via phosphatidylinositol 3-kinase/Akt- and MEK1/ERK-dependent pathways. *J Biol Chem.* 2002;277:19922-19928.
55. Moriarty N, Pandit A, Dowd E. Encapsulation of primary dopaminergic neurons in a GDNF-loaded collagen hydrogel increases their survival, re-innervation and function after intra-striatal transplantation. *Sci Rep.* 2017;7:1-14.
56. Adil MM, Vazin T, Ananthanarayanan B, et al. Engineered hydrogels increase the post-transplantation survival of encapsulated hESC-derived midbrain dopaminergic neurons. *Biomaterials* 2017;136:1-11.
57. Filippova A, Bonini F, Efremova L, et al. Neurothreads: development of supportive carriers for mature dopaminergic neuron differentiation and implantation. *Biomaterials* 2021;270.
58. Moriarty N, Parish CL, Dowd E. Primary tissue for cellular brain repair in Parkinson's disease: promise, problems and the potential of biomaterials. *Eur J Neurosci.* 2019;49:472-486.
59. Simão D, Silva MM, Terraso AP, et al. Recapitulation of human neural microenvironment signatures in iPSC-derived NPC 3D differentiation. *Stem Cell Rep.* 2018;11:552-564.
60. Pakkenberg B, Moller A, Gundersen HJG, et al. The absolute number of nerve cells in substantia nigra in normal subjects and in patients with Parkinson's disease estimated with an unbiased stereological method. *J Neurol Neurosurg Psychiatry.* 1991;54:30-33.
61. Hagell P, Brundin P. Cell survival and clinical outcome following intrastriatal transplantation in Parkinson disease. *J Neuropathol Exp Neurol.* 2001;60:741-752.
62. Tao Y, Vermilyea SC, Zammit M, et al. Autologous transplant therapy alleviates motor and depressive behaviors in parkinsonian monkeys. *Nat Med.* 2021;27:632-639.